ELSEVIER

Polymer 44 (2003) 1641–1645

polymer

www.elsevier.com/locate/polymer

Polymorphism of isotactic polybutene-1 as revealed by microindentation hardness. Part II: correlations to microstructure

F. Azzurri[a], A. Flores[b], G.C. Alfonso[a], I. Sics[c], B.S. Hsiao[c], F.J. Baltá Calleja[b,*]

[a]*Dipartimento di Chimica e Chimica Industriale, Via Dodecaneso 31, 16146 Genova, Italy*
[b]*Instituto de Estructura de la Materia, CSIC, Serrano 119, E-28006 Madrid, Spain*
[c]*Department of Chemistry, State University of New York, Stony Brook, NY 11974-3400, USA*

Abstract

The influence of polymorphism on the micromechanical properties of isotactic polybutene-1 (iPBu-1) has been investigated by means of the microhardness technique. Hardness data, H, of form I (hexagonal) are shown to be notably larger than those of form II (tetragonal). The H values of both polymorphic forms are shown to depend on the molecular weight, M_w, and the crystallization temperature, T_c. The hardness behaviour with M_w and T_c has been correlated to the changes of degree of crystallinity and nanostructure as derived from small angle X-ray scattering. The hardness values for iPBu-1 infinitely thick crystals (H_c^∞), of forms I and II, have been calculated for the first time. H_c^∞ of form I is shown to be notably larger than that of form II. This result is a consequence of the denser packing of the hexagonal crystal modification, and accounts for the large difference in H values found for forms I and II. Finally, the variation of the mechanical b-parameter, proportional to the surface-free energy of the crystals, with molecular weight is discussed.

Keywords: Isotactic polybutene-1; Polymorphism; Microhardness

1. Introduction

The basis of the microhardness technique lies on the local deformation produced at a microscopic scale on the material surface. Microindentation hardness is widely recognized to provide fundamental information on the morphology and microstructure of polymer materials [1–3]. It is now well established and experimentally supported that the microhardness of a semicrystalline polymer is intimately related to the degree of crystallinity, chain packing, crystal thickness and surface-free energy [1,4]. The sensitivity of microhardness to the polymer structural parameters makes this technique of great value in the study of the kinetics of solid state transformations such as those occurring upon crystallization from the glassy state or in the course of a polymorphic transition [5–9]. The influence of polymorphism on microhardness has been studied in isotactic polypropylene (iPP) [10]. Here, it was demonstrated that the microhardness technique can be successfully used to evaluate the amount of α and β phases within an iPP sample. Moreover, microindentation hardness has been applied to follow stress-induced polymorphic transitions such as those taking place in polybutylene terephthalate, its block copolymers and blends [7–9].

Isotactic polybutene-1 (iPBu-1) exhibits a tetragonal crystal cell (form II) when crystallized from the melt at atmospheric pressure [11]. This crystal modification is gradually transformed at room temperature into the thermodynamically favoured hexagonal form I [12,13]. This peculiar polymorphic transformation is completed after approximately 10 days annealing. Despite that the II → I transformation of polybutene-1 was recognized, its mechanism and the influence of polymorphism on the mechanical properties is still not fully understood.

This paper is the second of a series of two, concerning the study of the polymorphism of iPBu-1 by means of microindentation hardness. Part I was devoted to the study of the kinetics of the above-mentioned polymorphic transformation. This work describes the microhardness–microstructure correlations in both crystal modifications. The influence of molecular weight and crystallization temperature is discussed.

2. Basic equations

It is now widely accepted that the microhardness of a

* Corresponding author.

0032-3861/03/$ - see front matter © 2002 Elsevier Science Ltd. All rights reserved.
PII: S0032-3861(02)00864-9

semicrystalline polymer can be described in terms of a parallel model of alternating crystalline and amorphous regions in the following equation [1,4]:

$$H = H_c\alpha + H_a(1 - \alpha) \quad (1)$$

where H_c is the hardness of the crystals, H_a the hardness of the amorphous regions and α the fraction of the crystalline phase. The crystal hardness can be expressed in terms of [14]:

$$H_c = \frac{H_c^{\infty}}{1 + \frac{b}{l_c}} \quad (2)$$

where H_c^{∞} is the hardness of an infinitely thick crystal, l_c the crystal thickness, and b a parameter related to the surface-free energy of the crystal, σ_e, and to the energy required for plastic deformation of the crystal blocks, Δh, following [14]:

$$b = \frac{2\sigma_e}{\Delta h} \quad (3)$$

Eq. (2) describes the deviation of the crystal hardness from that of an infinitely thick crystal due to the limited size of the crystals and the occurrence of entanglements and defects located at their boundaries. On the other hand, the H_c^{∞} value is mainly controlled by chain packing.

3. Experimental

3.1. Materials

We used four different iPBu-1 grades with different molecular mass, within the range of 200,000 g/mol $\leq M_w \leq$ 850,000 g/mol, kindly supplied by Basell polyolefins, Louvain la Neuve (see Table 1). ^{13}C NMR analysis revealed that the fraction of isotactic pentads ($\approx$0.8) is independent of the molecular weight.

Quenched films were obtained by compression moulding as described in the preceding paper [15]. The final film thickness was of $\approx$300 μm. In addition, portions of the high molecular weight film (M_w = 850,000 g/mol) were isothermally crystallized at temperatures in the range of 80–110 °C (see Table 2), as described in detail in Ref. [15].

Table 1
Molecular weight, crystal modification, melting temperature, degree of crystallinity, long period, crystal thickness and microhardness values for the quenched samples with different molecular weight. The l_c data for form II were derived assuming $l_c(II) = l_c(I)/1.16$ (see the text)

Sample code	M_w (10^3 g/mol)	Crystal form	T_m (°C)	α	L (Å)	l_c (Å)	H (MPa)
PBu BR200	850	II	109.8	0.44	–	97	5.40
PBu 200	525	II	106.9	0.40	–	94	5.22
PBu 300	400	II	108.5	0.40	–	86	4.75
PBu 800	200	II	108.0	0.41	–	67	4.20
PBu BR200	850	I	119.8	0.43	262	112	34.3
PBu 200	525	I	116.9	0.40	273	109	22.4
PBu 300	400	I	115.9	0.38	262	99	21.4
PBu 800	200	I	117.0	0.39	196	78	26.4

3.2. Techniques

Differential scanning calorimetry (DSC), small angle X-ray scattering (SAXS) and microhardness (H) data for form II were obtained from measurements performed immediately after the samples were, either quenched from the melt, or isothermally crystallized. This procedure ensured that no incipient II → I transformation took place. The data for form I were obtained on samples where a complete transformation of form II into form I had occurred, according to our previous results [15].

DSC measurements were performed as described in the preceding paper [15]. Tables 1 and 2 summarize the melting temperature, T_m, and the degrees of crystallinity, α, of forms II and I, for the quenched and the isothermally crystallized samples, respectively. It is worth noting that the melting temperature of form I is about 10 °C higher than that of form II, in agreement with previous published work [16]. On the other hand, the α values (Eq. (1)) seem to remain constant upon the polymorphic transformation.

SAXS patterns were obtained using the synchrotron radiation source at the Advanced Polymers Beamline (X27C) in the National Synchrotron Light Source (NSLS), Brookhaven National Laboratory (BNL). Scattering patterns were recorded using a one-dimensional detector. A wavelength λ of 0.137 nm was used. The sample to detector distance was 193.5 cm. The data were corrected for the detector response and beam intensity. SAXS patterns were calibrated against a standard of silver behenate. Application of Bragg's law to the scattering maxima was used to calculate the long period, L. The crystal lamellar thickness, l_c, was estimated using the equation: $l_c = \alpha L$. The non-aged samples (form II) did not yield SAXS maxima. This is presumably due to the small electron density difference between the amorphous and the crystalline phase (ρ_a = 0.87 g/cm^3); (ρ_c = 0.91 g/cm^3) [13]. Thus, for the non-aged samples, we have assumed that $l_c(II) = l_c(I)/1.16$.

Table 2
Crystal modification, melting temperature, degree of crystallinity, long period, crystal thickness and microhardness values for the high molecular weight sample crystallized at different temperatures

T_c (°C)	Crystal form	T_m (°C)	α	L (Å)	l_c (Å)	H (MPa)
80	II	117.5	0.53	–	169	5.10
100	II	122.2	0.56	–	144	5.85
105	II	124.9	0.64	–	182	7.7
110	II	126.7	0.70	–	224	8.30
80	I	127.3	0.50	393	195	38.2
100	I	132.9	0.56	300	167	38.4
105	I	133.3	0.64	331	210	49.5
110	I	137.1	0.71	370	259	54.6

This assumption is based on the fact that the II → I transformation involves an extension of the 11/3 helical conformation (form II) into the 3/1 helix (form I). The ratio between the axial repeating units of this conformation is of 1.16. The above approximation seems reasonable, given that the overall mass degree of crystallinity remains constant upon the polymorphic transformation (see Tables 1 and 2).

Microhardness was measured at room temperature using a Leitz tester equipped with a Vickers diamond pyramid. Microhardness values, H, were derived from the optical measurement of the residual impression left behind upon load release, according to $H = 1.854P/d^2$, where d is the length of the indentation diagonal and P is the applied load. A loading cycle of 6 s was used in order to minimize the sample creep under the indenter. Loads of 49, 98 and 147 mN were employed to correct for the instant elastic recovery. For each load, at least eight measurements were averaged.

4. Results and discussion

4.1. Crystallinity dependence

Tables 1 and 2 summarize the values of T_m, α, L, l_c and H of forms II and I, for the quenched and isothermally crystallized samples, respectively. The H values of form I are shown to be remarkably higher than those of form II. This result is a consequence of the denser chain packing in the hexagonal crystal modification (form I) than that in the tetragonal crystal structure (form II) [17], as already discussed in the preceding paper [15]. The H variations with M_w (Table 1) and the conspicuous H-increase with increasing T_c (Table 2) can be explained in terms of the hardness dependence on α, l_c and the mechanical b-parameter (see Eqs. (1) and (2)), as will be discussed below.

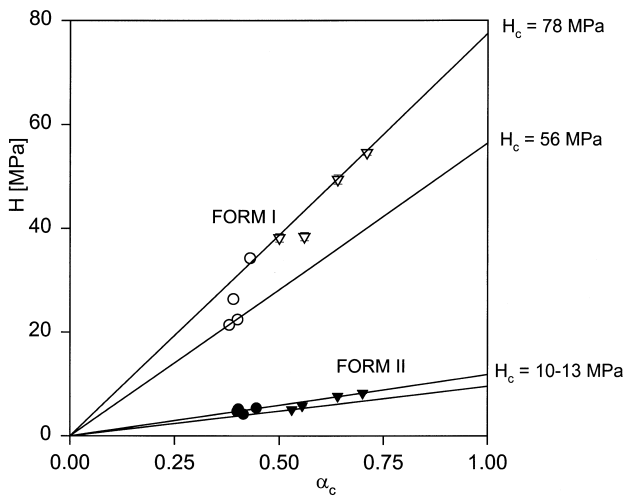

Fig. 1. Microhardness H of quenched (circles) and isothermally crystallized (triangles) iPBu-1 as a function of weight percent crystallinity: solid symbols (form II); open symbols (form I).

Fig. 1 illustrates the increase of H with α for forms II and I (solid and open symbols, respectively) for the quenched and the isothermally crystallized samples. One observes a tendency of H to increase with increasing α for both forms II and I. The straight lines in Fig. 1 follows the microhardness additivity law according to Eq. (1), where $H_a \approx 0$, since the glass transition temperature of iPBu-1 is below room temperature. In the case of form II, the crystal hardness values, calculated using Eq. (1) and represented in Fig. 1 as the intercept with the right-hand y-axis, lie in the range of 10–13 MPa. On the other hand, H_c values for samples in form I lie in the range of 56–78 MPa. The spread in the H_c values of form II and I could be attributed to the changes in the thickness of the lamellar crystals (Eq. (2), Tables 1 and 2). The microhardness–lamellar thickness correlation is discussed in detail below.

4.2. Influence of lamellar thickness

4.2.1. Hardness for infinitely thick crystals (form II) for quenched samples

In order to discuss the influence of lamellar thickness with crystal hardness, it is convenient to rewrite Eq. (2) as:

$$\frac{1}{H_c} = \frac{1}{H_c^{\infty}}\left(1 + \frac{b}{l_c}\right) \tag{4}$$

In this way, we can derive the H_c^{∞} and b values from a linear plot of $1/H_c$ versus $1/l_c$. Fig. 2 shows this plot for the quenched samples with different molecular weights in form II. From this analysis, a b value of 110 Å and $H_c^{\infty} = 27$ MPa are obtained. While the b value obtained lies in the range of those reported in the literature for other polymers [18], it is interesting to note the low H_c^{∞} value derived for form II of iPBu-1, in contrast to those reported in other systems (e.g., for polyethylene oxide, $H_c^{\infty} = 150$ MPa; for polyethylene, $H_c^{\infty} = 170$ MPa and for polyethylene terephthalate,

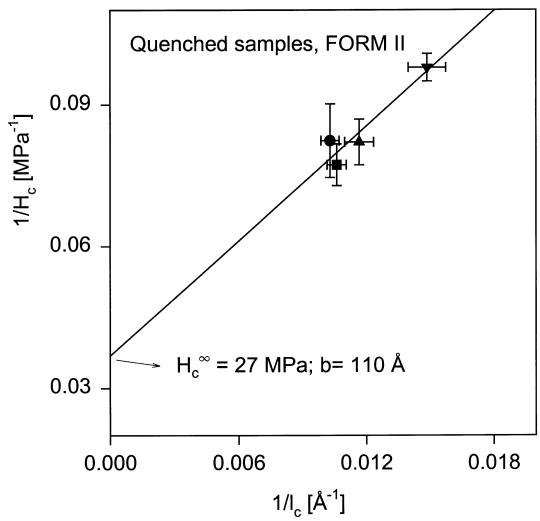

Fig. 2. Plot of $1/H_c$ versus $1/l_c$ for the samples of iPBu-1, measured immediately after quenching: (●) 850,000 g/mol; (■) 525,000 g/mol; (▲) 400,000 g/mol; (▼) 200,000 g/mol.

$H_c^\infty = 392$ MPa [1]). This is probably due to the low value of the chain packing density within the crystals ($\rho_c = 0.91$ g/cm^3).

4.2.2. Comparison of mechanical parameters between forms I and II: for isothermally crystallized samples

Fig. 3 presents the plot of $1/H_c$ versus $1/l_c$ for the high molecular weight sample, crystallized at different temperatures at the beginning and after the end of the polymorphic transformation (forms II and I, respectively). The data for form II have been fitted to a straight line, assuming $H_c^\infty = 27$ MPa (Fig. 2). The b value obtained in this case ($b = 260$ Å) is significantly larger than the one derived for the quenched samples ($b = 110$ Å, Fig. 2). The b-parameter is known to be proportional to the surface-free energy of the crystals (Eq. (3)). Hence, crystals developed in the course of an isothermal crystallization seem to contain a larger number of defects and molecular entanglements at their surface boundary, with respect to the crystals developed during quenching from the melt. In other words, during isothermal crystallization, defects are segregated more efficiently to the crystalline–amorphous interphase. Similar results have previously been reported for polyethylene samples quenched and slowly crystallized from the melt [18].

Concerning the linear fit of data form I (Fig. 3), results yield values of $H_c^\infty = 104$ MPa and $b = 78$ Å. It is noteworthy the high H_c^∞ value of form I with respect to that derived for form II ($H_c^\infty = 27$ MPa). This result supports our foregoing contentation, that the remarkable enhancement observed in the H values upon the II → I transformation (see Fig. 1) is mainly attributed to the different chain packing and hence to different H_c^∞ values in both crystal modifications.

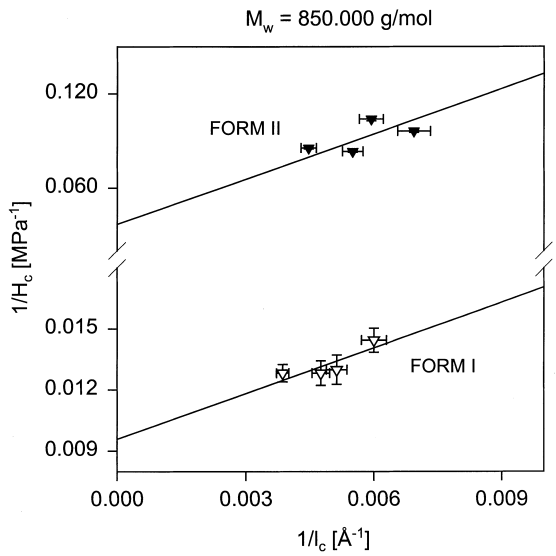

Fig. 3. Plot of $1/H_c$ versus $1/l_c$ for the highest molecular weight sample of iPBu-1. Solid symbols (form II); open symbols (form I).

4.3. Influence of molecular weight (form I): the role of the b-parameter

In the preceding section, a H_c^∞ value of 104 MPa has been derived for the isothermally crystallized samples of form I (see Fig. 3). Assuming the same H_c^∞ value for the quenched samples, we have obtained the b values for the various molecular weights (see Table 3). Fig. 4(a) illustrates the variation of the b-parameter with the molecular weight of the samples in form I. One can see an initial b-increase with increasing M_w, followed by a conspicuous drop in the b values for the high molecular weight sample. The initial b-rise could be attributed to an increase in the entanglement density at the crystal surface with increasing chain length. A similar b-behaviour with M_w has been reported for polyethylene samples in a wide range of molecular weights ($56{,}000 \le M_\eta \le 173{,}000$ g/mol) [18]. On the other hand, the significant decrease in the b value for the high molecular weight sample could be explained in terms of an increasing number of tie molecules interconnecting adjacent crystals. This number would tend to increase with increasing molecular weight.

4.4. Relationship between the mechanical b-parameter and the thermodynamic b^*-parameter

In a previous study, we suggested the analogy between Eq. (2) and the Thomson–Gibbs equation [19]. While the former equation describes the crystal hardness depression due to the finite size of the crystals and the mechanical parameter b, the latter expresses the melting temperature dependence upon l_c:

$$T_m = T_m^\infty\left(1 - \frac{b^*}{l_c}\right) \tag{5}$$

where T_m^∞ is the equilibrium melting temperature and b^* is a thermodynamic parameter, related to σ_e and to the equilibrium heat of fusion Δh_f^∞ ($b = 2\sigma_e/\Delta h_f^\infty$).

Fig. 4(b) illustrates the variation of the b^*-parameter, as derived from calorimetric measurements, as a function of molecular weight, for quenched samples (form I) (Table 3). We have assumed that the T_m^∞ value of form I of iPBu-1 is about 10 K higher than that of form II [16], where the latter value was derived from Marand's approach [20,21]. Fig. 4(b) reveals that the b^*-parameter values follow the same trend as that shown in Fig. 4(a) for the b-parameter. This result supports that the change in b with M_w is a

Table 3
Calculated values for the b and b^* parameters and the ratio between them for quenched samples of iPBu-1 crystallized at $T_c = 20$ °C as a function of molecular weight, M_w

M_w (10^3 g/mol)	b (Å)	b^* (Å)	b/b^*
850	35	7.5	4.7
525	94	8.1	11.5
400	84	6.8	12.3
200	42	4.4	9.5

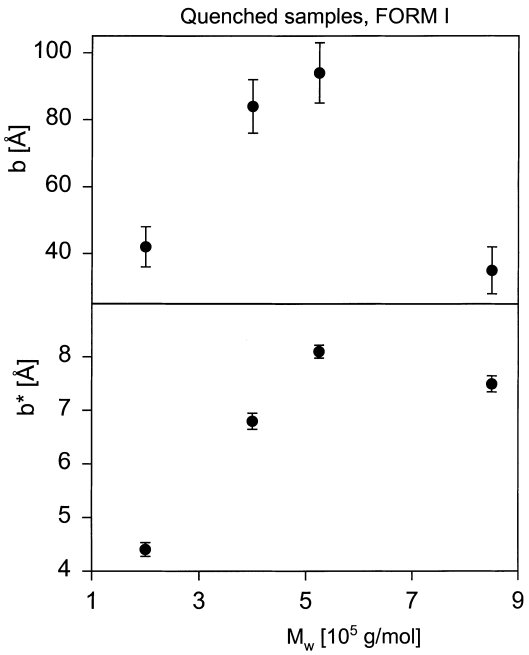

Fig. 4. Variation of the b and b^* parameters with molecular weight for quenched samples of iPBu-1 measured at the end of the II → I transformation.

consequence of the variation of the surface-free energy, which is a function of molecular mass. It is noteworthy the low b^* values with respect to the high b data. This result has already been observed for other polymers and suggests that the energy required for plastic deformation of the crystals is significantly lower than the enthalpic changes due to melting. Finally, it is to be noted that the ratio b/b^* does not remain constant but first increases and then decreases with molecular weight (see Table 3). The reason for this is that the b-parameter increases and decreases faster with M_w than the b^*-parameter.

5. Conclusion

1. The hardness values of the tetragonal and the hexagonal crystal modifications of isotatic polybutene-1 are shown to be a function of, both, molecular weight and crystallization temperature. This is a consequence of the variation of the degree of crystallinity and the thickness of the lamellae with M_w and T_c.
2. From the analysis of the $1/H_c$ versus $1/l_c$ plot, it is possible to derive the crystal hardness of an infinitely thick crystal H_c^∞ for both forms I and II. Results reveal that H_c^∞ for form II ($H_c^\infty = 104$ MPa) is substantially larger than that for form I ($H_c^\infty = 27$ MPa).
3. Analysis of the microhardness–nanostructure correlation for the high molecular weight sample crystallized at different temperatures shows that the mechanical parameter b is significantly larger than that derived for the quenched samples. This result could be attributed to a more efficient segregation of the defects and entanglements to the crystalline–amorphous interphase for the isothermally crystallized samples.
4. We found that the b value is constant at the beginning of the transformation (form II), while for the completely transformed material (form I), b shows an initial increase with increasing molecular weight, followed by a conspicuous drop for the high molecular weight.

Acknowledgements

Grateful acknowledgement is due to the MCYT, Spain (Grant BFM2000-1474) and to the COST P1 'Soft Condensed Matter' program of the EU for the generous support of this investigation. The Stony Brook group gratefully thanks the financial support of US National Science Foundation (DMR-0098104). One of the authors (AF) is also grateful to the Comunidad Autónoma de Madrid for the award of a postdoctoral grant.

References

[1] Baltá Calleja FJ, Fakirov S. Microhardness of polymers. Cambridge: Cambridge University Press; 2000.
[2] Bajpaj R, Keller JM, Datt SF. Makromol Chem 1988;20/21:465.
[3] Evans BL. J Mater Sci 1989;24:173.
[4] Baltá Calleja FJ. Trends Polym Sci 1994;2:419.
[5] Baltá Calleja FJ, Santa Cruz C, Asano T. J Polym Sci, Polym Phys 1993;31:557.
[6] Kajaks J, Flores A, García Gultiérrez MC, Rueda DR, Baltá Calleja FJ. Polymer 2000;41:7769.
[7] Faikrov A, Boneva D, Baltá Calleja FJ, Krumova M, Apostolov AA. J Mater Sci Lett 1998;17:453.
[8] Apostolov AA, Boneva D, Baltá Calleja FJ, Krumova M, Faikrov S. J Macromol Sci Phys B 1998;37:543.
[9] Boneva D, Baltá Calleja FJ, Fakirov S, Apostolov AA, Krumova M. J Appl Polym Sci 1998;69:2271.
[10] Baltá Calleja FJ, Martinez Salazar J, Asano T. J Mater Sci Lett 1998; 7:165.
[11] Natta G, Corradini P. Nouvo Cimento Suppl 1960;15:9.
[12] Boor J, Mitchell JC. J Polym Sci 1962;62:70.
[13] Fogila AJ. Appl Polym Symp 1969;11:1.
[14] Baltá Calleja FJ, Kilian HG. Colloid Polym Sci 1985;263:697.
[15] Azzurri F, Flores A, Alfonso GC, Baltá Calleja FJ. Macromolecules 2002;35:9069.
[16] Danusso F, Gianotti G. Makromol Chem 1964;80:1.
[17] Danusso F, Gianotti G. Makromol Chem 1963;61:139.
[18] Bayer RK, Baltá Calleja FJ, Kilian HG. Colloid Polym Sci 1997;275: 432.
[19] Baltá Calleja FJ, Santa Cruz C, Asano T, Sawatari C. Macromolecules 1990;23:5352.
[20] Marand H, Xu J, Srinivas S. Macromolecules 1998;31:8219.
[21] Xu J, Srinivas S, Marand H. Macromolecules 1998;31:8230.